Bioelectrocatalytic System Coupled with Enzyme-Based Biocomputing Ensembles Performing Boolean Logic Operations: Approaching "Smart" Physiologically Controlled Biointerfaces

ARTICLE *in* ACS APPLIED MATERIALS & INTERFACES · JANUARY 2009

Impact Factor: 6.72 · DOI: 10.1021/am800088d · Source: PubMed

6 AUTHORS, INCLUDING:

Marcos Pita
Spanish National Research Council
85 PUBLICATIONS **2,875** CITATIONS
SEE PROFILE

Maryna Ornatska
Clarkson University
28 PUBLICATIONS **1,373** CITATIONS
SEE PROFILE

ARTICLE

Bioelectrocatalytic System Coupled with Enzyme-Based Biocomputing Ensembles Performing Boolean Logic Operations: Approaching "Smart" Physiologically Controlled Biointerfaces

Jian Zhou, Tsz Kin Tam, Marcos Pita, Maryna Ornatska, Sergiy Minko,* and Evgeny Katz*

Department of Chemistry and Biomolecular Science and NanoBio Laboratory (NABLAB), Clarkson University, Potsdam, New York 13699-5810

ABSTRACT The modified electrode for electrocatalytic oxidation of NADH was developed using a pH-switchable redox interface. The operation of the modified electrode was controlled by logic operations performed by enzyme systems processing biochemical input signals. The electrocatalytic oxidation of NADH was activated upon appropriate combinations of the signals processed by the **AND/OR** logic operations performed by the enzymes. The modified interface was reset in a mute nonactive state by another enzyme reaction. The coupling between the enzyme logic systems and the bioelectrocatalytic interface was achieved by pH changes produced in situ by the enzyme reactions, resulting in different protonation states of the polymeric matrix associated with the electrode surface. The bioelectrocatalytic system integrated with biochemical computing systems opens the way to novel "smart" interfaces for multisignal biosensors and signal-controlled biofuel cells. In a long perspective, this approach will allow physiological control of implantable bioelectronic devices.

KEYWORDS: switchable interface • enzyme logic • switchable biolectrocatalysis • "smart" interface • signal-responsive material • modified surface

1. INTRODUCTION

Bioelectrocatalytic systems based on chemically modified electrodes have important applications in biosensors (1−3) and biofuel cells (4−6). Recent attention to the bioelectrocatalytic systems with variable on-demand properties has resulted in the development of switchable biocatalytic electrodes responding to chemical (7, 8), optical (9, 10), or magnetic (11, 12) external signals controlling the activity of the systems. Signal-responsive biocatalytic electrodes have been suggested as components of switchable biosensors (13, 14), biofuel cells (15), or chemical memory units (16). Various approaches based on applications of controlled switchable interfaces activated by different stimuli could be used to design signal-controlled biomolecular-functionalized surfaces (17). Usually, the activity of signal-responsive bioelectrocatalytic systems is controlled by a special kind of external signal (e.g., light, magnetic field, or pH change), allowing reversible transitions from active to inactive states and back. Some of the studied systems may respond to two kinds of physical or physical/chemical signals (e.g., the potential applied to the electrode and illumination (16) or the pH change and illumination (18)); however, none of the designed systems is capable of responding to several biochemical signals applied simultaneously.

Recent research activity in unconventional chemical computing (19) resulted in the development of various chemical systems processing information and performing Boolean logic operations in response to several chemical input signals (20, 21). Novel horizons were opened in the chemical computing research area upon the introduction of biochemical systems and formulation of biomolecular computing (biocomputing) concepts (22, 23). The biocomputing systems benefit from highly specific biocatalytic or biomolecular-recognition reactions proceeding simultaneously in multicomponent ensembles, where the individual steps are complementary and the reacting components are compatible. Multicomponent enzyme systems aimed at preparing substrates for the analytical steps or eliminating cross-reacting substances interfering with the analysis were studied a long time ago (going back to 1960−1970s) (24); however, they have never been considered as elements of logic operations mimicking electronic computing processes. Recently pioneered enzyme-based logic gates are able to process biochemical input signals upon performing various Boolean operations (**AND**, **OR**, **XOR**, **INHIB**, etc,) and generate a single output signal as a result of the biocomputing process (25). Further development of the enzyme-based logic gates allowed their assembly in biocomputing networks composed of several concatenated gates performing sequences of logic operations upon acceptance of many

* To whom all correspondence should be addressed. Fax: 1-315-2686610 (Department). Tel.:1-315-2684421(E.K.), 1-315-2683807(S.M.). E-mail: ekatz@clarkson.edu (E.K.), sminko@clarkson.edu (S.M.).

Received for review September 29, 2008 and accepted November 3, 2008

DOI: 10.1021/am800088d

Published on Web 11/24/2008

biochemical input signals (26, 27). For example, a series of three concatenated logic gates (**OR**−**AND**−**XOR**) could accept four different biochemical signals in 16 different combinations, processing them according to the built-in Boolean logic and generating one final output signal dependent on the combination of all input signals (26). Enzyme−logic networks are able to perform complex logic operations, for example, an **IMPLICATION** function when the output signal is controlled not only by the values of the input signals but also by their correct or incorrect order (27). Enzymes were applied as input signals activating biocomputing systems and resulting in various logic operations (28). The advantage of the enzyme-input-controlled logic systems is the application of the input signals in a low catalytic quantity and the possibility of using enzyme inputs in the form of immobilized materials. The enzyme-input-controlled logic gates could be scaled up to at least 10 units in a logic network upon appropriate optimization of the system (29). The coupling of biocomputing systems, specifically enzyme-based logic gates or their networks, with signal-responsive biocatalytic interfaces would allow "smart" bioelectrochemical systems controlled by many biochemical signals to come simultaneously and be processed logically according to the built-in Boolean program.

The present paper addresses a new approach to the "smart" biocatalytic interfaces controlled by Boolean logic operations performed in situ by enzymatic systems.

2. EXPERIMENTAL SECTION

Chemicals and Materials. All chemicals were purchased from Sigma-Aldrich and used as supplied: 4,4′-dimethoxy-2,2′-bipyridine (dmo-bpy), $(NH_4)_2OsCl_6$, poly(4-vinylpyridine) (P4VP; MW 160 kDa), (bromomethyl)dimethylchlorosilane, and 1,4-dihydro-β-nicotinamide adenine dinucleotide (NADH), β-D-(+)-glucose, urea, sucrose, ethyl butyrate, glucose oxidase (**GOx**) from *Aspergillus niger*, type X-S (E.C. 1.1.3.4); esterase (**Est**) from *porcine liver* (E.C. 3.1.1.1), crude; invertase (**Inv**) from *Baker's yeast*, grade VII (E.C. 3.2.1.26); and urease from *jack beans* (E.C. 3.5.1.5). Ultrapure water (18 M$\Omega \cdot cm^{-1}$) from a NANOpure Diamond (Barnstead) source was used in all of the experiments. Indium/tin oxide (ITO) conductive glass (20 ± 5 Ω/sq) was purchased from Aldrich and used as a working modified electrode. The synthesis of $Os(dmo\text{-}bpy)_2Cl_2$ was performed according to the published procedure (30). P4VP was functionalized with $Os(dmo\text{-}bpy)_2$ pendant groups in a solution, and then the redox polymer was grafted onto the ITO electrode surface according to the procedure published in detail elsewhere (31). Shortly, the ITO electrode was reacted in toluene with 0.1% (v/v) (bromomethyl)dimethylchlorosilane for 20 min at 70 °C. Then the silanized ITO glass was reacted with Os-complex-functionalized P4VP in toluene (10 mg $\cdot$ mL^{-1}) to yield the redox-modified electrode.

Electrochemical Measurements. Electrochemical measurements were performed with an ECO Chemie Autolab PSTAT 10 electrochemical analyzer using the software package GPES 4.9 (General Purpose Electrochemical System) for the voltamperometric measurements and the FRA 4.9.007 (Frequency Response Analyzer) for the faradaic impedance measurements. The measurements were performed with a three-electrode system in a standard cell (ECO Chemie), using the Os−P4VP-modified ITO working electrode (geometrical area 1.2 cm^2), a Metrohm Ag|AgCl|KCl 3 M as the reference electrode, and a Metrohm Pt wire as the counter electrode. The measurements were carried out at an ambient temperature (23 ± 2 °C). The faradaic impedance spectra were recorded while applying a bias potential of 0.4 V and using a 5 mV alternative voltage in the frequency range 10 mHz to 10 kHz. The experimental impedance spectra were fitted using electronic equivalent circuits (Randles and Ershler model) in order to derive the electron-transfer resistance, R_{et}, values (32). For this purpose, commercial software (ZView, version 2.1b, Scribner Associates, Inc.) was employed.

Composition of Logic Gates and Input Signals. The **AND** gate machinery was defined as a 10 mL aqueous solution including 0.1 M sodium sulfate, 0.15 M sucrose, and dissolved oxygen in equilibrium with air. Input **A** of the **AND** gate was 100 units of Inv, and input **B** was 60 units of GOx. The **OR** gate machinery was defined as a 10 mL aqueous solution containing 0.1 M sodium sulfate, 0.01 M ethyl butyrate, 0.01 M glucose, and dissolved oxygen in equilibrium with air. Input **A** was 50 units of Est, and input **B** was 50 units of GOx. The machinery for the **Reset** function was 10 mL of a 0.1 M sodium sulfate solution including 30 mM urea. The trigger for the **Reset** function was an input signal of 50 units of urease. The **Reset** function was combined with two logic gates (**AND**/**OR**) to get the resettable logic gates by combining both machineries in the same volume. All logic gates operated at room temperature and in equilibrium with air. All concentrations of the substrates mentioned above and the amounts of the enzyme inputs were optimized to produce a significant $|\Delta pH|$, yielding clearly distinguished "**0**" and "**1**" states.

Logic Gate Action. To record the logic gates action, the machinery solution of each system was monitored with a pH meter (SevenEasy, Mettler-Toledo Inc.) at room temperature. Being a nonbuffered solution, the system requires an equilibration time to achieve a constant pH value. This value was taken as (**0**, **0**) input. Inputs **A** and **B** were added to the system in all different combinations (**0**, **1**; **1**, **0**; **1**, **1**) to get the results that correspond to the possible truth table combinations. The pH values were recorded continuously during the whole experiment. The same procedure was performed for the **AND** gate, the **OR** gate, and the **Reset** trigger. Cyclic voltammograms and faradaic impedance spectra were recorded prior to the logic gate operations and after completion of the respective biochemical reactions.

3. RESULTS AND DISCUSSION

Recently, we reported on a polymer brush-modified electrode with the electrochemical activity of the polymer-bound redox groups controlled by pH values (31). The P4VP brush was grafted on an ITO electrode with a low density of polymeric chains, ca. 0.075 chain $\cdot$ nm^{-2}. Prior to attachment to the electrode surface, the polymer was functionalized with redox-active $Os(dmo\text{-}bpy)_2^{2+}$ (dmo-bpy = 4,4′-dimethoxy-2,2′-bipyridine) groups bound to the polymer through their complexation with the pyridine ligands. Low loading of the osmium complex on the polymer brush (ca. 4 complex units per polymer chain; ca. 1 osmium complex per 350 pyridine units) resulted in long average distances between the redox species, preventing direct electron exchange between them (31). A reversible electrochemical process for the redox polymer grafted on the electrode surface was observed only at pH < 4.5 when the polymer is protonated (positively charged) and swollen, and the chains are flexible. The electron exchange between the redox species and the electrode surface proceeded in a quasi-diffusional mode, allowing short distances for the electron-transfer processes when flexible polymer chains were com-

Scheme 1. Logic Operations AND/OR Performed by the Enzyme-Based Systems Resulting in the ON and OFF States of the Bioelectrocatalytic Interface Followed by the Reset Function To Complete the Reversible Cycle[a]

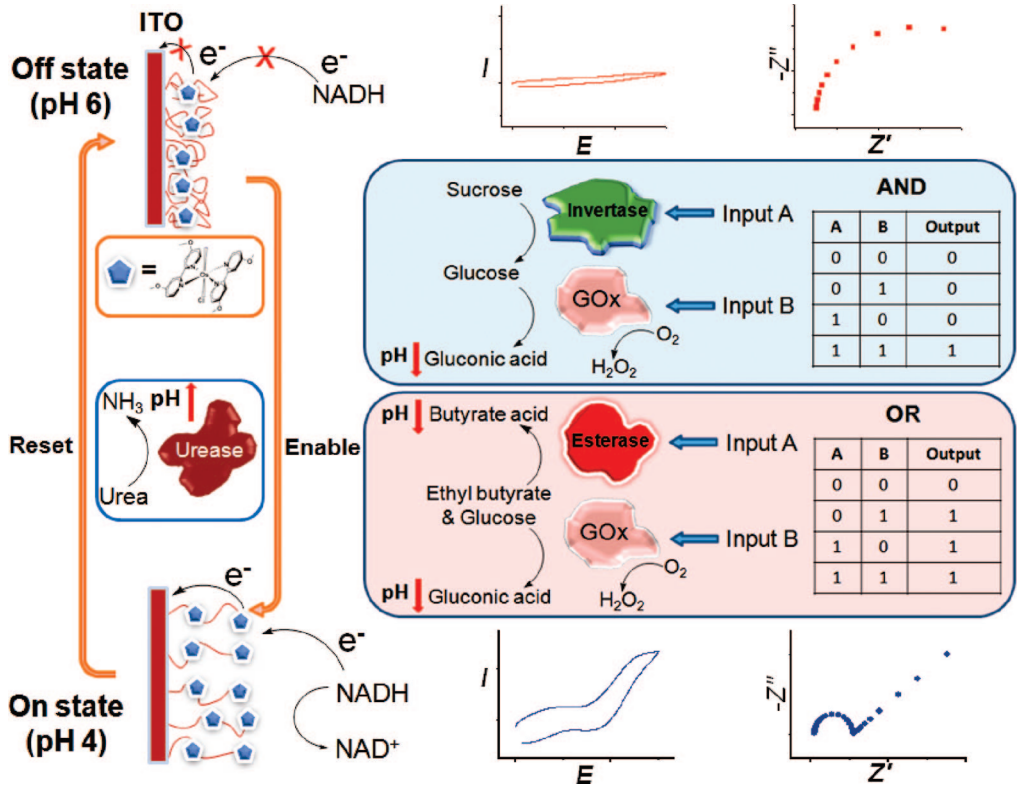

[a] Schematically shown cyclic voltammograms and impedance spectra correspond to the **ON** and **OFF** states of the bioelectrocatalytic electrode.

ing to the electrode surface upon random translocations. At pH > 5, the polymer becomes deprotonated (neutral) and shrunken, and the movements of the polymer chains are "frozen" because of the dense packing of the hydrophobic chains. In this state, the electron exchange is inhibited because of the long distances separating the redox species from each other and from the electrode surface. Therefore, the modified electrode demonstrated the reversible redox process, $E° = 0.28$ V (vs Ag/AgCl reference electrode), at pH = 4.0, while the electrochemical process was switched off at pH = 6 (31). The reversible switching ON and OFF was demonstrated for the modified electrode by the stepwise application of background solutions with pH ~ 4 and 6, respectively.

Because the studied redox interface is pH-switchable, we designed enzyme-based logic gates using enzymes as biocatalytic input signals, processing information according to the Boolean operations **AND** or **OR**, and generating pH changes (acidification) as the output signal from the gates (Scheme 1). The **AND** gate performed a sequence of biocatalytic transformations: sucrose hydrolysis was biocatalyzed by invertase (Inv, input **A**), producing glucose, which was oxidized by oxygen in the presence of glucose oxidase (GOx, input **B**). The later reaction resulted in the formation of gluconic acid and therefore lowered the solution pH value. The absence of the enzymes was considered as the input signals "**0**", while their presence in the operational concentrations (10 units · mL^{-1} for Inv and 6 units · mL^{-1} for GOx) was interpreted as the input signals "**1**". The biocatalytic reaction chain was activated only in the presence of both enzymes (Inv and GOx) (input signals "**1**, **1**"), resulting in the lowering of the initial pH ~ 6.3 to pH ~ 4.2 (ΔpH > 0.5 was considered as the output signal "**1**"). The absence of either of the two enzymes (input signals "**0**, **1**" or "**1**, **0**") or both of them (input signals "**0**, **0**") resulted in inhibition of the gluconic acid formation, and thus no pH changes were observed (ΔpH < 0.1 was considered as the output signal "**0**"; Figure 1A). Thus, the biocatalytic chain mimics the **AND** logic operation expressed by the standard truth table showing the output signal dependence on the combinations of the input signals **A** and **B** (Scheme 1). Another gate operating as a Boolean **OR** function was composed of two parallel reactions: hydrolysis of ethyl butyrate and oxidation of glucose biocatalyzed by esterase (Est, input **A**; 5 units · mL^{-1}) and glucose oxidase (GOx, input **B**; 5 units · mL^{-1}) and resulting in the formation of butyric acid and gluconic acid, respectively (Scheme 1). Any of the produced acids and both of them together resulted in a lowering of initial pH ~ 5.5 to a value of pH ~ 3.5. Thus, in the absence of both enzymes (Est and GOx) (input signals "**0**, **0**"), both reactions were inhibited and the pH value was unchanged (ΔpH < 0.1; output signal "**0**"). In the presence of any of the enzymes (Est or GOx; input signals "**0**, **1**" or "**1**, **0**") or both of them together (input signals "**1**, **1**"), one of the reactions or both of them proceeded and resulted in the acidification of the solution (ΔpH > 0.5; output signal "**1**"; Figure 1B). The features of the system correspond to the **OR** logic operation and can be expressed by the standard truth table showing

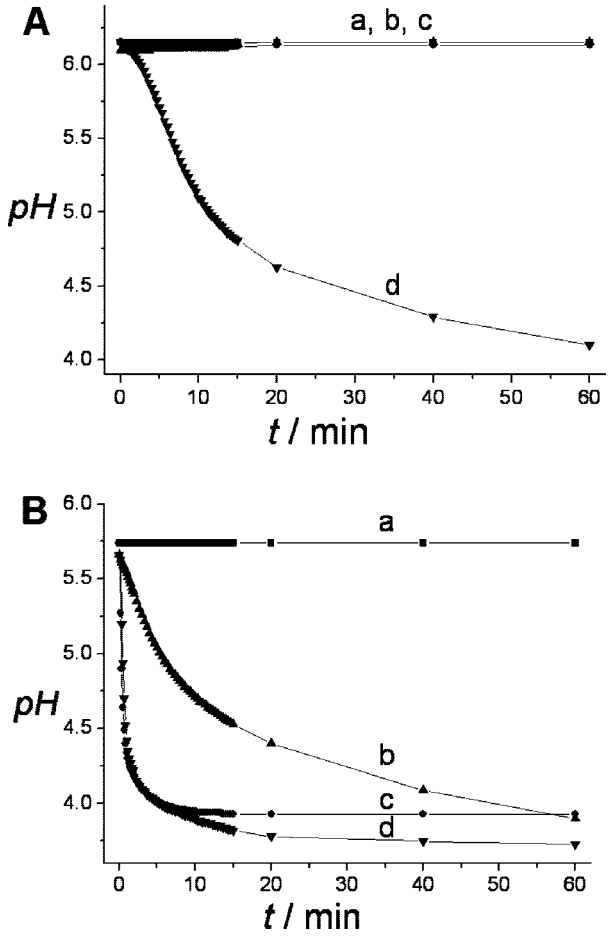

FIGURE 1. In situ pH changes induced by the enzyme logic systems (A) AND logic gate and (B) OR logic gate, upon the application of different combinations of input signals: (a) 0, 0; (b) 0, 1; (c) 1, 0, and (d) 1, 1.

the output signal dependence on the combinations of the input signals **A** and **B** (Scheme 1).

Upon completion of the enzyme reactions resulting in the logically controlled acidic medium (pH = 3.5−4.2), the pH value can be reset to the initial value (pH ∼ 5.5−6.3) by the formation of ammonia upon hydrolysis of urea biocatalyzed by urease (Scheme 1). Thus, the **Reset** function was activated by the input signal composed of urease (5 units · mL^{-1}).

It should be noted that the pH changes in the range of 0.5 > ΔpH > 0.1 were considered as digitally undefined, in the same way as an electrical signal in electronic logic gates is undefined while being between two threshold limits. Variation of the enzyme concentrations between zero and operational values (between "**0**" and "**1**" input signals) results in a surface-response function of the logic gates, which can be used for the optimization of the gate performance (29); this was outside the scope of the present study.

In situ logically processed (**AND**/**OR**) enzyme signals resulting in the acidic pH value enabled the redox process of the polymer-modified electrode interface, while the **Reset** function yielded an almost neutral pH value and switched it off. The electrochemically reversible redox process of the immobilized osmium complex enabled at the acidic pH

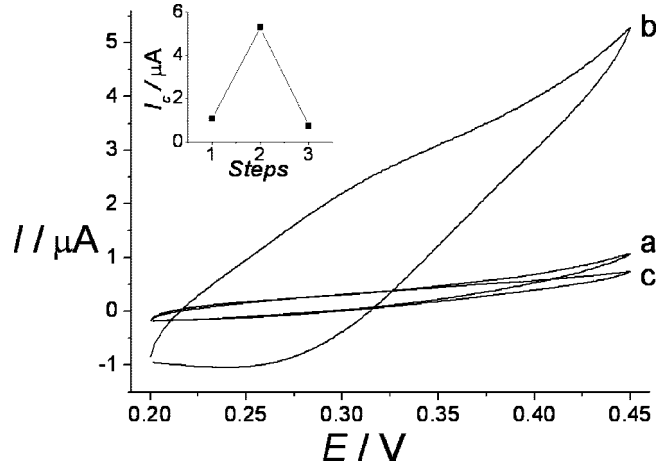

FIGURE 2. Cyclic voltammograms obtained for the biocatalytic electrode in the presence of 0.5 mM NADH: (a) OFF-state, (b) ON-state, (c) after application of the Reset function. Inset: Reversible changes of the electrocatalytic current (E = 0.45 V) upon logically controlled Enable/Reset functions. The experiment was performed with a potential scan rate of 10 mV · s^{-1}.

value was used to activate electrocatalytic oxidation of NADH. Modified electrodes functionalized with various redox species (33), including those modified with osmium complexes similar to the redox complex used in the present study (34, 35), have shown to be effective electrocatalysts for the oxidation of NADH. When the solution pH was reset to the almost neutral value upon the urease input, the redox activity of the modified electrode was switched off and the secondary electrocatalytic oxidation of NADH was inhibited (Scheme 1).

The electrocatalytic oxidation of NADH by the logically enabled modified electrode was studied by cyclic voltammetry and faradaic impedance spectroscopy upon the application of different combinations of the enzyme input signals applied in situ. Figure 2 shows typical cyclic voltammograms obtained in the presence of NADH (0.5 mM) recorded when the pH-switchable electrode is in the **ON-state** at pH ∼ 4.1, curve b, and when it is in the **OFF-state** at pH ∼ 6.2, curves a and c. The **ON-state** clearly demonstrates the electrocatalytic oxidation of NADH at potentials larger than the redox potential of the osmium complex, $E°$ = 0.28 V (pH = 4). The **OFF-state** does not show any electrocatalytic activity because the redox process of the osmium complex is inhibited. It should be noted that the capacitance of the modified electrode was also dramatically changed upon variation of the pH value between 6.2 and 4.1, reflecting restructuring of the polymeric thin film from the shrunken state to the swollen state and demonstrating low and high interfacial capacitance, respectively. Figure 3 shows typical impedance spectra in the form of Nyquist plots obtained in the presence of NADH (0.5 mM) recorded when the pH-switchable electrode is in the **ON-state** at pH ∼ 4.1, curve b, and when it is in the **OFF-state** at pH ∼ 6.2, curves a and c. The **OFF-state** demonstrates a high electron-transfer resistance, R_{et}, of ca. 250 kΩ derived from the corresponding impedance spectra, thus reflecting the inhibition of the electrocatalytic process. The **ON-state** shows a low R_{et} value of ca. 50 kΩ corresponding to the proceeding electrocatalytic

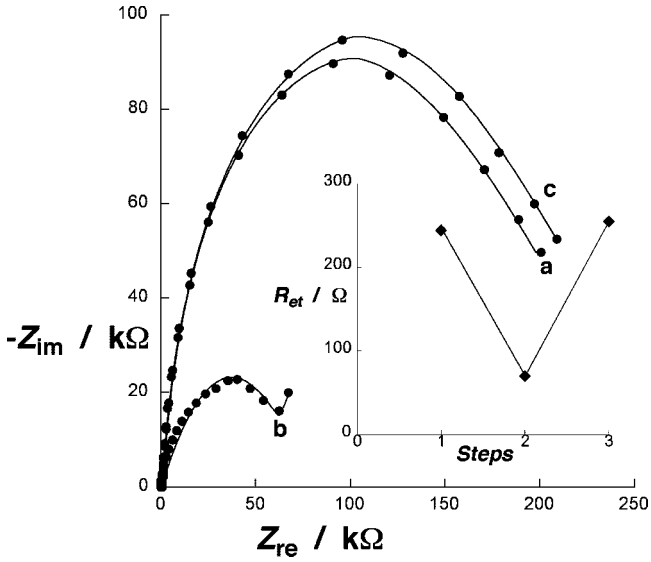

FIGURE 3. Faradaic impedance spectra obtained for the biocatalytic electrode in the presence of 0.5 mM NADH: (a) OFF-state; (b) ON-state; (c) after application of the Reset function. Inset: Reversible changes of the electron-transfer resistance upon logically controlled Enable/Reset functions. The experiment was performed upon application of the biasing potential of 0.4 V.

oxidation of NADH. The impedance spectra correlate with the cyclic voltammetry measurements, and they give a quantitative interpretation of the **ON/OFF** states in terms of the resistances, similarly to the circuitries of the logic gates used in electronics. A control experiment performed in the absence of NADH and in the presence of all other components of the enzyme logic systems (e.g., in the presence of GOx and glucose) does not show the changes in the cyclic voltammogram and impedance spectra observed in the presence of NADH and corresponding to the development of the electrocatalytic anodic current. Only much smaller changes (not observable on the scale currently used) corresponding to the switching **ON/OFF** of the osmium complex redox process (31) were observed in the control experiment.

The experiments were always started at pH = 6 ± 0.5 when the redox electrode is in the **OFF-state**, showing no electrocatalytic current and a high electron-transfer resistance [Figure 2 (curve a) and Figure 3 (curve a), respectively]. A nonbuffered background solution, 0.1 M sodium sulfate, included dissolved sucrose (0.15 M) and oxygen in the case of the **AND** logic gate or glucose (0.01 M), ethyl butyrate (0.01 M), and oxygen in the case of the **OR** logic gate. In both cases, urea (30 mM) was included in the solution for the **Reset** function. After the cyclic voltammogram and impedance spectrum were recorded, combinations of the enzyme input signals (**0**, **0**; **0**, **1**; **1**, **0**; **1**, **1**) were applied and changes of the pH value were registered (Figure 1). Depending on the logic gate used (**AND/OR**) and controlled by the combination of applied enzyme inputs, the pH value of the solution stayed unchanged or decreased, reaching the acidic value pH = 3.5−4.2 when the redox process was enabled. This resulted in the activation of the electrocatalytic oxidation of NADH reflected by the appearance of the anodic electrocatalytic current in the cyclic voltammogram and by the low value of R_{et} in the impedance spectra. It should be noted that the cyclic voltammogram [Figure 2 (curve b)] and the impedance spectrum [Figure 3 (curve b)], corresponding to the **ON-state** of the electrode, represent averaged typical results that can be obtained upon various combinations of the enzyme input signals enabling the redox process. Specifically, the **ON-state** was achieved by application of **1**, **1** enzyme input signals in the case of the **AND** logic gate and by the application of **0**, **1**, **1**, **0**, and **1**, **1** enzyme input signals in the case of the **OR** logic gate. After the logic operation was completed and if the pH value was alternated, we applied the urease input to activate the **Reset** function and to return the system to the original **OFF-state**. The cyclic voltammogram and impedance spectrum were returned to the initial form, corresponding to the **OFF-state** of the system. It should be noted that frequently the impedance spectrum obtained upon the reset process demonstrated R_{et} even larger than the original value, because the pH was reaching values higher than the initial pH, thus resulting in even stronger inhibition of the redox process. The combination of the **Enable/Reset** functions allowed the cyclic switching **ON** and **OFF** of the bioelectrocatalytic process controlled by the enzyme logic operations [Figures 2 and 3 (insets)]. In order to make multiple cycles of activation/deactivation of the bioelectrocatalytic system, the modified electrode was washed from the used enzyme logic system and immersed in a new solution to repeat the **Enable/Reset** cycle upon the addition of new combinations of biochemical input signals.

4. CONCLUSIONS AND PERSPECTIVES

The obtained result shows for the first time that bioelectrocatalytic processes routinely used in electrochemical biosensors and biofuel cells can be controlled by the biocomputing systems performing logic operations. Keeping in mind that the enzyme logic gates can be scaled up to computing networks composed of several (potentially many) concatenated logic gates, we can predict the possibility of various bioelectronic devices logically controlled by biochemical and even complex physiological processes. This opens a new perspective for "smart" interfacing of bioelectronic devices with biological systems. In a long perspective, this approach will allow physiological control of implantable bioelectronic devices. The future "smart" bioelectronic devices will include the enzyme logic networks organized in microfluidic systems, allowing efficient delivery of the biochemical signals to the "decision-making" enzyme logic elements and then rinsing to reset the system. The rate of the "decision-making" processes will correlate with the biochemical/physiological changes in the body, thus allowing effective administration of drug delivery and implantable device operation. The biochemical information processing elements (e.g., enzymes operating as the signal processing species rather than the input signals) will be immobilized at the signal-responsive interfaces and/or in the channels of the microfluidic systems. Some preliminary experiments demonstrated that local changes (e.g., pH changes) generated in situ by the immobilized enzyme logic systems could be used to switch/tune signal-responsive interfaces (see the Supporting Information). Biocomputing/enzyme logic elements even

of moderate complexity could allow effective interfacing between complex physiological processes and implantable biomedical devices, providing autonomous, individual, "upon-demand" medical care, which is the objective of the new nanomedicine concept (36, 37). Various logically controlled bioelectronic systems based on a similar approach, including multisignal responsive biosensors and biochemical actuating systems, biochemically switchable/tunable biofuel cells, and bioelectronic chips, are underway in our laboratory.

Acknowledgment. This research was supported by NSF grants "Signal-Responsive Hybrid Biomaterials with Built-in Boolean Logic" (Grant DMR-0706209) and "Biochemical Computing: Experimental and Theoretical Development of Error Correction and Digitalization Concepts" (Grant CCF-0 726698). An award from the Semiconductor Research Corp., "Cross-disciplinary Semiconductor Research" (Grant 2008-RJ-1839G), is gratefully acknowledged. T.K.T. gratefully acknowledges a Wallace H. Coulter scholarship from Clarkson University.

Supporting Information Available: An example of the enzyme logic system coupled with a signal-responsive bioelectronic interface based on the immobilized enzymes. This material is available free of charge via the Internet at http://pubs.acs.org.

REFERENCES AND NOTES

(1) Willner, I.; Katz, E. *Angew. Chem., Int. Ed.* **2000**, *39*, 1180–1218.
(2) Wang, J. *Chem. Rev.* **2008**, *108*, 814–825.
(3) Wollenberger, U.; Spricigo, R.; Leimkuhler, S.; Schronder, K. In *Biosensing for the 21 st Century*; Renneberg, R.; Lisdat, F., Eds.; Book Series Advances in Biochemical Engineering/Biotechnology; Springer: Berlin, 2008; Vol. 109, pp 19—64.
(4) Katz, E.; Shipway, A. N.; Willner, I. In *Handbook of Fuel Cells—Fundamentals, Technology, Applications*; Vielstich, W.; Gasteiger, H.; Lamm, A., Eds.; Wiley: Chichester, U.K., 2003; Vol. 1, Part 4, Chapter 21, pp 355—381.
(5) Davis, F.; Higson, S. P. J. *Biosens. Bioelectron.* **2007**, *22*, 1224–1235.
(6) Barton, S. C.; Gallaway, J.; Atanassov, P. *Chem. Rev.* **2004**, *104*, 4867–4886.
(7) Mir, M.; Katakis, I. *Mol. Biosyst.* **2007**, *3*, 620–622.
(8) Willner, I.; Lion-Dagan, M.; Katz, E. *Chem. Commun.* **1996**, 623–624.
(9) Katz, E.; Willner, B.; Willner, I. *Biosens. Bioelectron.* **1997**, *12*, 703–719.
(10) Yan, P.; Holman, M. W.; Robustelli, P.; Chowdhury, A.; Ishak, F. I.; Adams, D. M. *J. Phys. Chem. B* **2005**, *109*, 130–137.
(11) Katz, E.; Baron, R.; Willner, I. *J. Am. Chem. Soc.* **2005**, *127*, 4060–4070.
(12) Loaiza, Ó. A.; Laocharoensuk, R.; Burdick, J.; Rodríguez, M. C.; Pingarron, J. M.; Pedrero, M.; Wang, J. *Angew. Chem., Int. Ed.* **2007**, *46*, 1508–1511.
(13) Katz, E.; Willner, I. *Chem. Commun.* **2005**, 4089–4091.
(14) Wang, J. *Electroanalysis* **2008**, *20*, 611–615.
(15) Katz, E.; Willner, I. *J. Am. Chem. Soc.* **2003**, *125*, 6803–6813.
(16) Baron, R.; Onopriyenko, A.; Katz, E.; Lioubashevski, O.; Willner, I.; Wang, S.; Tian, H. *Chem. Commun.* **2006**, 2147–2149.
(17) Liu, Y.; Mu, L.; Liu, B. H.; Kong, J. L. *Chem.—Eur. J.* **2005**, *11*, 2622–2631.
(18) Doron, A.; Portnoy, M.; Lion-Dagan, M.; Katz, E.; Willner, I. *J. Am. Chem. Soc.* **1996**, *118*, 8937–8944.
(19) Adamatzky, A.; De Lacy Costello, B.; Asai, T. *Reaction—Diffusion Computers*; Elsevier Science: Amsterdam, The Netherlands, 2005.
(20) (a) De Silva, A. P.; Uchiyama, S. *Nat. Nanotechnol.* **2007**, *2*, 399–410. (b) Pischel, U. *Angew. Chem., Int. Ed.* **2007**, *46*, 4026–4040.
(21) Credi, A. *Angew. Chem., Int. Ed.* **2007**, *46*, 5472–5475.
(22) Head, T. *New Gener. Comput.* **2001**, *19*, 301–312.
(23) Shao, X. G.; Jiang, H. Y.; Cai, W. S. *Prog. Chem.* **2002**, *14*, 37–46.
(24) *Immobilized enzymes. Current state and perspectives*; Berezin, I. V.; Antonov, V. K.; Martinek, K. M., Eds.; Moscow State University Publishing: Moscow, 1976.
(25) Baron, R.; Lioubashevski, O.; Katz, E.; Niazov, T.; Willner, I. *J. Phys. Chem. A* **2006**, *110*, 8548–8553.
(26) Niazov, T.; Baron, R.; Katz, E.; Lioubashevski, O.; Willner, I. *Proc. Natl. Acad. U.S.A.* **2006**, *103*, 17160–17163.
(27) Strack, G.; Ornatska, M.; Pita, M.; Katz, E. *J. Am. Chem. Soc.* **2008**, *130*, 4234–4235.
(28) Strack, G.; Pita, M.; Ornatska, M.; Katz, E. *ChemBioChem* **2008**, *9*, 1260–1266.
(29) Privman, V.; Strack, G.; Solenov, D.; Pita, M.; Katz, E. *J. Phys. Chem. B* **2008**, *112*, 11777–11784.
(30) Taylor, C.; Kenausis, G.; Katakis, I.; Heller, A. *J. Electroanal. Chem.* **1995**, *396*, 511–515.
(31) Tam, T. K.; Ornatska, M.; Pita, M.; Minko, S.; Katz, E. *J. Phys. Chem. C* **2008**, *112*, 8438–8445.
(32) Katz, E.; Willner, I. *Electroanalysis* **2003**, *15*, 913–947.
(33) Katakis, I.; Dominguez, E. *Mikrochim. Acta* **1997**, *126*, 11–32.
(34) Storrier, G. D.; Takada, K.; Abruña, H. D. *Inorg. Chem.* **1999**, *38*, 559–565.
(35) Popescu, I. C.; Dominguez, E.; Narvaez, A.; Pavlov, V.; Katakis, I. *J. Electroanal. Chem.* **1999**, *464*, 208–214.
(36) Seetharam, R. N. *Curr. Sci.* **2006**, *91*, 260.
(37) Briquet-Laugier, V.; Ott, M. O. *Biofutur* **2006**, *265*, 57–62.

AM800088D